УДК 622:528.7
DOI 10.52575/2712-7443-2024-48-4-542-564

LULC Dynamics and Carbon Sequestration in Major Iron Ore Regions of Russia and China

Lihua Huang
Belgorod State National Research University,
85 Pobedy St, Belgorod 308015, Russia
E-mail: lhhuang0@163.com

Abstract. This study examines the dynamics of land use/land cover (LULC) and carbon sequestration in Lebedinsky and Stoylensky mining and processing plants (LGOK and SGOK) located in iron ore regions of Russia and the Anshan-Benxi iron ore region of China from 1985 to 2020. Through spatial analysis and estimation of carbon sequestration by vegetation and its deposition by soils, the impact of mining activities, urban expansion, and ecological restoration efforts on regional land use patterns and carbon sequestration capacities were assessed. The results reveal significant LULC transformations in both regions, primarily driven by mining development and urbanization. In Russia, cropland area decreased by approximately 8 % (640.78 km²), largely replaced by construction land and forest, with forest cover rising from 12.69 % to 16.69 %, indicating effective ecological management. Conversely, in China, stronger development pressures led to a decrease in forest cover from 40.44 % to 36.73 % and an increase in construction land from 5.62 % to 12.51 %. Carbon sequestration analysis revealed contrasting trends: while the total carbon sequestration in the Russian mining regions remained stable, with a slight increase of 3.69 megatons (Mt), the total carbon sequestration in the Chinese mining regions declined significantly by 31.41 Mt, primarily due to reductions in forest and grassland carbon sequestration. These findings underscore the need for sustainable development that balances economic growth and ecological stability in mining regions. Implementing effective strategies such as afforestation, wetland restoration, and adaptive land-use policies is essential to mitigate the environmental impacts of mining and to sustain carbon sequestration. Future policies should prioritize harmonizing industrial growth with environmental conservation to promote sustainable land use in heavily industrialized areas.

Keywords: Land use/land cover (LULC) dynamics; Carbon sequestration; Iron ore mining regions; Sustainable land management

For citation: Huang L. 2024. LULC Dynamics and Carbon Sequestration in Major Iron Ore Regions of Russia and China. Regional geosystems, 48(4): 542–564. DOI: 10.52575/2712-7443-2024-48-4-542-564

Динамика LULC и поглощения углерода в основных регионах железорудных месторождений России и Китая

Хуан Л.
Белгородский государственный национальный исследовательский университет
Россия, 308015, Белгород, ул. Победы 85
E-mail: lhhuang0@163.com

Аннотация. В исследовании анализируется динамика землепользования / наземного покрова (LULC) и поглощения углерода в районах добычи железной руды Лебединского и Стойленского горно-обогатительных комбинатов в России и областях железорудного производства Аньшань и Бэньси в Китае с 1985 по 2020 год. С помощью пространственного анализа и оценки секвестрации углерода растительностью и депонирование его почвами определено влияние горной промышленности, урбанизации и усилий по экологическому восстановлению на характер землепользования и способность к поглощению углерода. Результаты показывают значительные изменения в использовании земли в обеих областях, в основном обусловленные увеличением добычи полезных

ископаемых и ростом городов. В России площадь сельскохозяйственных угодий уменьшилась примерно на 8 % (640,78 км²), что связано с застройкой территории и расширением лесных площадей. При этом увеличение лесного покрова с 12,69 % до 16,69 % указывает на эффективное экологическое управление. Промышленное развитие в горнорудном районе Китая, напротив, привело к уменьшению лесного покрова с 40,44 % до 36,73 % и увеличению площади застроенных территорий с 5,62 % до 12,51 %. Анализ углеродных депозитов показал противоположные тенденции: в то время как общая способность к поглощению углерода в российских районах добычи железной руды осталась стабильной, с небольшим увеличением на 3,69 Мт, в китайских железорудных районах эта величина значительно уменьшилась (на 31,41 Мт), в основном из-за снижения углеродопоглощения лесами и травянистыми угодьями. Эти результаты подчеркивают необходимость устойчивого развития, которое создает баланс между экономическим ростом и экологической стабильностью в горнорудных районах. Реализация эффективных стратегий, таких как озеленение, восстановление болот и адаптивные политики землепользования, является критически важной для снижения экологических последствий добычи полезных ископаемых и сокращения выбросов диоксида углерода.

Ключевые слова: динамика землепользования / наземного покрова (LULC), поглощение углерода, регионы добычи железной руды, устойчивое землепользование

Для цитирования: Huang L. 2024. LULC Dynamics and Carbon Sequestration in Major Iron Ore Regions of Russia and China. Regional geosystems, 48(4): 542–564. DOI: 10.52575/2712-7443-2024-48-4-542-564

Introduction

Iron ore mining regions are pivotal to the economies of both Russia and China, particularly due to their contributions to global iron ore supply and the associated environmental impacts. Russia, holding over 58.3 billion tons of iron ore reserves in categories A+B+C1, ranks among the world's top reserve holders, alongside Brazil and Australia [Shvidenko, Nilsson, 2003; Кирсанов, 2023]. China, though fourth in iron ore reserves, is the world's leading steel producer, accounting for over 54 % of global steel output in 2023[3]. This high production volume, however, relies on lower-grade domestic ores, resulting in increased carbon dioxide emissions – a challenge that underscores the environmental costs of China's steel industry and highlights the need for sustainable practices [Pan et al., 2011; Pang et al., 2023].

Assessing land use and land cover (LULC) changes in iron ore-affected regions of Russia and China is essential for understanding the ecological impacts of mining and promoting sustainable resource management [Wohlfart et al., 2017]. Russia's Kursk Magnetic Anomaly (KMA) iron ore province, with extensive reserves concentrated in Belgorod and Kursk regions, exemplifies long-term landscape transformations due to industrial activity, particularly in mines like the Lebedinsky and Stoylensky complexes [Гзогян С., Гзогян Т., 2018]. Similarly, China's Xianshan iron mine, expected to become the country's largest by 2027, highlights China's strategic efforts to reduce reliance on imported iron ore through domestic exploration and extraction[4] [Wu et al., 2016]. Despite differences in resource quality and industry structure, these two countries' iron ore industries exhibit significant potential for mutual economic collaboration, such as the proposed resource alliances to stabilize global mineral markets [Seto et al., 2012]. Coordinated management efforts could also help mitigate environmental degradation, which is a growing concern for both countries as mining activities increasingly transform landscapes and disrupt local ecosystems [Grimm et al., 2008].

[3] China to boost coal output, reserves to ensure power supply – NDRC. Reuters. March 7, 2022. URL: https://www.reuters.com/business/energy/china-boost-coal-output-reserves-ensure-power-supply-ndrc-2022-03-05/ (Accessed: 12.09.2024).

[4] Xi'anshan Iron Mine: To build a world-class underground iron ore mine and help the "cornerstone plan" of China's iron and steel industry. 2024. Electronic resources. (in Chinese). URL: https://ln.chinadaily.com.cn/a/202409/30/WS66fa40a5a310b59111d9c368.html (accessed: 12.09.2024)

Monitoring changes in land composition using Landsat images, visual and automated interpretation methods is widely used at different scales [Shelestov et al., 2017, Alshari, Gawali, 2021, Basheer et al., 2022, Ahialey et al., 2024], but there are still prospects for increasing the detection accuracy using an automated method for processing space images [Pirnazar et al., 2021, Беленко, Accex, 2022]. Recently, land use / land cover (LULC) classification has been actively supplemented using the accuracy attained from different models [Abbas et al., 2021, Digra et al., 2022, Yifter et al., 2022, Rengma, Yadav, 2024]. The contribution of the computer hierarchical system developed by FAO specialists [Di Gregorio, Jansen, 2006] is highly appreciated for land cover classification, as it is based on the biophysical characteristics of land cover. However, this classification does not assume the allocation of mixed classes of land cover, and when moving to the map legend, such mixed classes can be reflected on the maps [Савин, Березуцкая, 2024].

This study investigates LULC changes and their effects on carbon sequestration within 20 km of major mining areas in Russia and China from 1985 to 2020, leveraging remote sensing (RS) and geographic information system (GIS) technologies [Xu et al., 2024]. Using data from the Chinese Academy of Sciences' Aerospace Information Research Institute's 30-meter-resolution dataset (GLC_FCS30 1985_2020), this analysis classifies land cover into seven types – Cropland, Forest, Grassland, Wetland, Water body, Bareland, and Construction land – using ArcGIS 10.8.1 [Zhang et al., 2021]. Key analytical methods include land use transition matrices, land use dynamic models, and carbon sequestration estimation techniques, which provide a robust framework for evaluating long-term ecological impacts [Zheng et al., 2024].

In summary, this paper aims to advance the understanding of LULC dynamics and their effects on carbon sequestration in major mining regions of Russia and China. By applying detailed RS and GIS methodologies, it not only assesses ecological transformations within the 20 km zones around the mining sites but also provides critical insights that support policy development for ecological restoration and sustainable resource management in these regions.

Materials and methods

Study Area

This study focuses on the LGOK and SGOK mining areas located within the Kursk Magnetic Anomaly (KMA) region in Russia, as well as the Anshan-Benxi iron ore mining areas situated in Liaoning Province, China. The study areas are defined as zones extending 20 km outward from the boundaries of the mining sites.

The LGOK and SGOK mining areas are located in the Kursk Magnetic Anomaly. This region experiences a temperate continental climate, characterized by cold, snowy winters and warm, humid summers. The annual average temperature ranges from 5°C to 7°C, with winter (January) averages of –7°C to –8°C and summer (July) averages around 19°C to 21°C. Average annual precipitation is between 500 and 600 mm, with most rainfall occurring during the summer months. The surrounding terrain is primarily flat plains with occasional rolling hills.

The Anshan-Benxi mining areas are distributed in Liaoning Province, China. The region features a temperate continental monsoon climate with distinct seasons. The annual average temperature ranges from 7°C to 9°C, with winter (January) averages of –10°C to –15°C and summer (July) averages of 24°C to 26°C. Annual precipitation is between 700 and 1000 mm, with over 70 % occurring during the rainy season (June to August). The terrain around the mining areas is mostly represented by hills and low mountains.

Data collection

The LULC data used in this study for the years 1985, 1990, 1995, 2000, 2005, 2010, 2015, and 2020 were sourced from the Global 30-meter Fine Ground Cover Dynamic Monitoring Product (GLC_FCS30 1985_2020) [Zhang et al., 2021], provided by the Aerospace Information Research Institute of the Chinese Academy of Sciences. This dataset, covering the period

from 1985 to 2020, offers a spatial resolution of 30m x 30m. Following standardized land use classification systems [Anderson, 1976; Di Gregorio, 2005; Савин, Березуцкая, 2024], the original data were reclassified in ArcGIS 10.8.1 into seven primary land use types: Cropland, Forest, Grassland, Wetland, Water Body, Bareland, and Construction Land (Table 1). This reclassification ensured consistency and comparability with established methodologies for LULC studies [Turner et al., 1995; Foley et al., 2005; Lambin, Geist, 2008].

Table 1
Таблица 1

LULC type definition
Определение видов землепользования/наземного покрова

LULC	Definition
Cropland	paddy fields, irrigated dry land, rain-fed dry land, vegetable plots.
Forest	evergreen broadleaf forest, deciduous broadleaf forest, evergreen needleleaf forest, deciduous needleleaf forest, and mixed forest.
Grassland	grasslands, meadows, savannas, desert steppes, and urban artificial grasslands.
Wetland	inland swamps, lake swamps, river floodplains, forest/shrub wetlands, peat bogs, mangroves, salt marshes, etc., which are located at the junction of land and water.
Water body	water-covered areas such as rivers, lakes, reservoirs, and ponds.
Bareland	land cover types with less than 10% vegetation coverage, such as deserts, sandy areas, gravelly areas, bare rocks, saline-alkaline soils.
Construction land	urban areas, roads, rural cottages, and mines, which are primarily based on asphalt, concrete, sand and stone, bricks, glasses, and other materials.

Land Use Transfer Matrix Analysis

The land use transfer matrix is a widely used analytical tool to quantify and visualize the direction and magnitude of transitions between different land use types over a specific period and spatial scale [Pontius, Malanson, 2005]. This matrix provides a comprehensive view of land use change dynamics, reflecting the flow and interaction of land use types during the study period [Lambin et al., 2003]. In this study, the raster calculator tool in ArcGIS 10.8.1 software is utilized to overlay the land use raster data layers from the beginning (period t1) and the end (period t2) of the study. This process calculates the areas of mutual transitions between different land use types within the study area. The formula is as follows:

$$A_{ij} = \begin{bmatrix} A_{11} & \cdots & A_{1n} \\ \vdots & \ddots & \vdots \\ A_{n1} & \cdots & A_{nn} \end{bmatrix}$$

where A_{ij} is the area transferred from land use type i (at the start of the study) to land use type j (at the end of the study) during the study period, and n is the total number of land use types.

Land Use Dynamics Index

The Land Use Dynamics Index (K) measures the changes a specific land use type within a defined time range on the site under study [Liu et al., 2005; Lambin, Geist, 2008]. A higher K value indicates more significant changes and lower stability, while a lower K value reflects less significant changes and higher stability. The formula is as follows:

$$K = \frac{U_b - U_a}{U_a} \times \frac{1}{T} \times 100\%$$

where U_a and U_b are the areas of a specific land use type at the beginning and end of the study, respectively; T is the the study duration (in years).

Comprehensive land-use dynamics (S) illustrate the overall intensity of land use changes, reflecting transitions among all land use types during the study period [Verburg et al., 2004; Turner et al., 2007]. A higher S value indicates more intense changes. The formula is:

$$S = \left(\sum_{i=1}^{n} \frac{\Delta U_{i-j}}{U_i}\right) \times \frac{1}{T}$$

where $^{\Delta U_{i-j}}$ is the total area converted from land use Type *i* to Type *j* during the period *T*; U_i is the area of land use Type *i* at the beginning of the study.

Carbon Sink Estimation

The carbon sink capacity of mining area ecosystems refers to their net carbon absorption, primarily driven by two mechanisms: the absorption of carbon by vegetation and soil, particularly in forests, grasslands, and croplands, through photosynthesis that produces organic matter [Lal, 2004; Ni, 2013] and artificial carbon inputs from land reclamation efforts [Post, Kwon, 2000]. However, this study excludes the latter due to the unavailability of data and its limited relevance.

Based on previous research and vegetation and soil carbon density values for various land use types (see Table 1) [Zhang et al., 2012], the carbon sequestration for the research area is estimated using the formula:

$$P_c = S \times \left(C_{C\ vegetation} + C_{C\ soil}\right)$$

where P_c is the carbon sequestration of a single land-use type, in t; S is the area of a certain land-use type, in hm^2; C_c is the vegetation or soil carbon density of a certain land-use type, in Mg/hm^2.

Results and discussion

Land use/land cover classification

From 1985 to 2020, the LGOK and SGOK iron ore affected areas in Russia and the Anshan-Benxi iron ore affected areas in China experienced significant spatiotemporal changes in land use/land cover (LULC). These changes reflect both anthropogenic influences, such as mining expansion and urbanization, and natural ecological processes [Liu et al., 2023]. The study shows that land use changes were driven by various factors, including mining activities [Rasskazov et al., 2023], infrastructure expansion, and ecological protection policies [Hu et al., 2024], which displayed regional characteristics. The previously obtained results of mapping the structure of the land fund in the zone with a radius of 20 km from LGOK and SGOK [Корнилов и др., 2015] were associated with the result of classification according to seven LULC types [Хуан, Полетаев, 2024], which made it possible to verify the data obtained by different methods.

Tables 1 and 2 summarize the area (km^2) and proportion (%) changes across seven major land use types: cropland, forest, grassland, wetland, water body, bareland, and construction land. Additionally, LULC distribution maps (Fig. 1 and 2) visually illustrate the spatial distribution and dynamic transitions, highlighting the adaptation of land use in different areas.

Table 2
Таблица 2

Carbon intensity of different land use types (Mg/hm^2)
Углеродоемкость различных видов землепользования (Мг/ гм^2)

LULC	Forest	Grassland	Cropland
Vegetation	86	21	5
Soil	189	116	95

In Russia's LGOK and SGOK regions, cropland area declined significantly, decreasing from 53.23 % (4264.68 km²) in 1985 to 45.24 % (3623.90 km²) in 2020, providing an overall reduction of around 8 % (Fig. 3). Forest area notably increased from 12.69 % (1016.40 km²) in 1985 to 16.69 % (1337.35 km²) in 2020, especially in the post-2000 period, indicating a potential shift towards ecological restoration and natural vegetation regeneration. Grassland areas, though showing minor fluctuations, remained relatively stable, increasing from 28.90 % to 30.05 %, with most expansion occurring near mining peripheries. Wetland and water body areas showed minimal but stable recovery; wetlands expanded from 0.06 % (4.45 km²) in 1985 to 0.11 % (8.79 km²) in 2020. Construction land doubled in area, from 3.97 % (317.70 km²) in 1985 to 6.60 % (528.41 km²) by 2020, reflecting infrastructure demands related to mining activities.

Fig. 1. Geographical location of LGOK and SGOK iron ore mining areas of Russia
Рис. 1. Географическое положение месторождений железной руды ЛГОК и СГОК в России

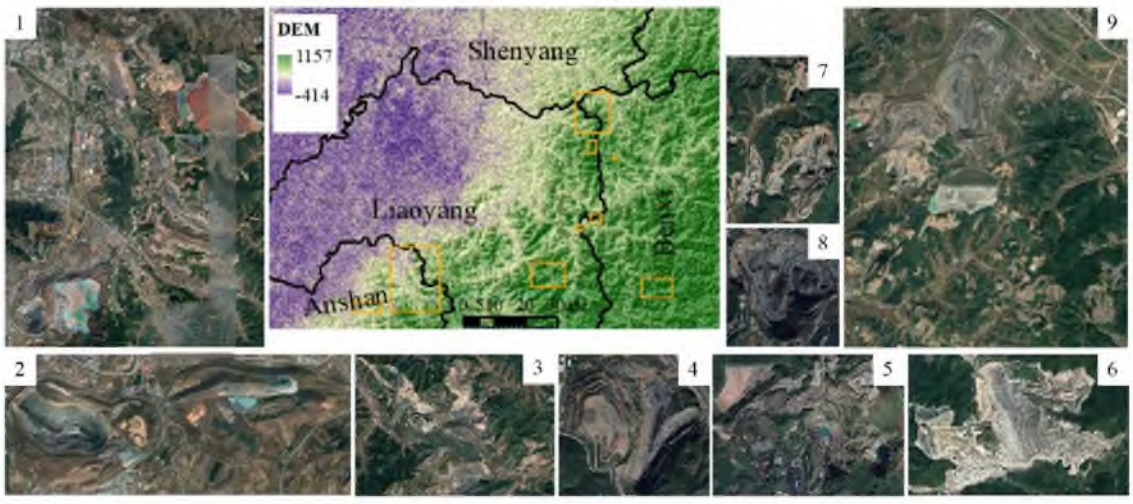

Fig. 2. Geographical location of Anshan-Benxi iron ore mining areas of China
Рис. 2. Географическое положение районов добычи железной руды Аньшань-Бэньси в Китае

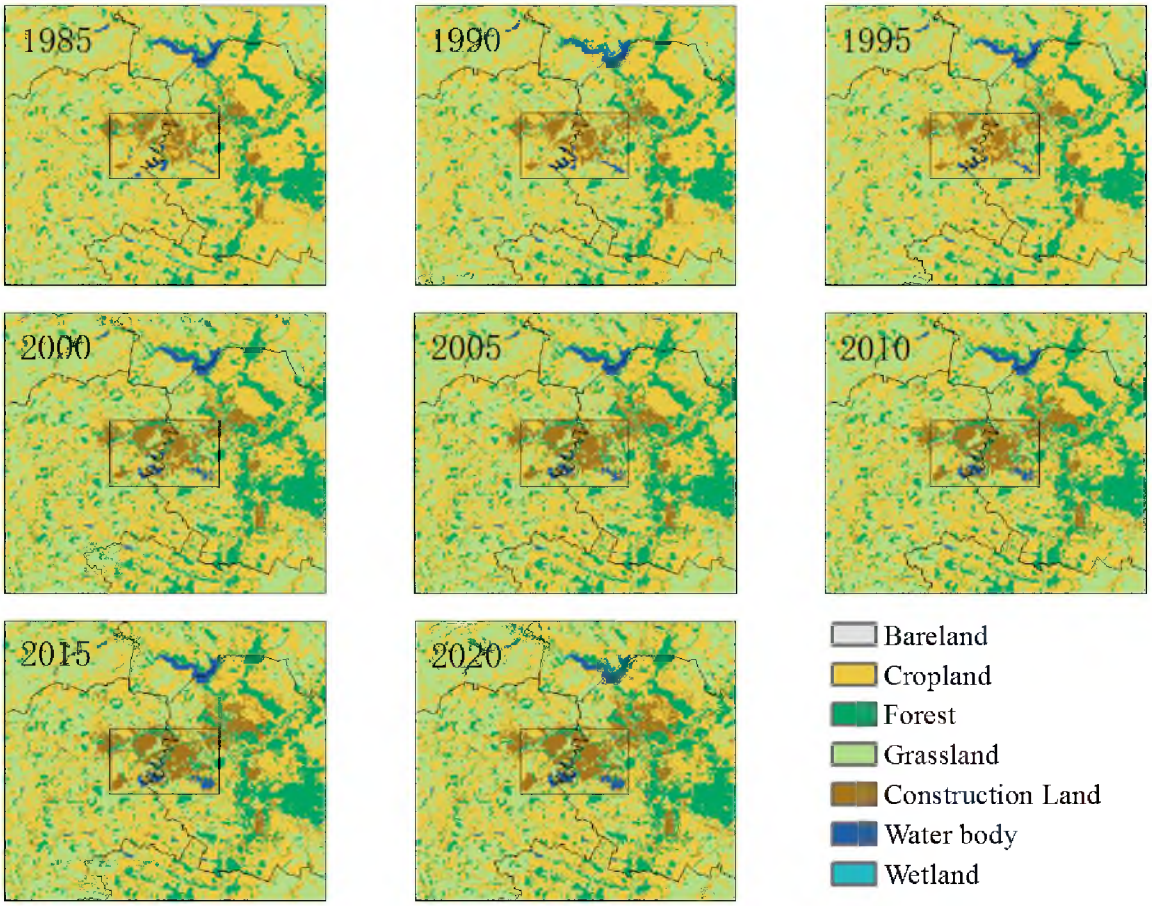

Fig. 3. LULC distribution map of the affected area of LGOK and SGOK Iron Ore Mine
Рис. 3. Карта распределения землепользования / наземного покрова
в зоне воздействия железорудного производства (ЛГОК и СГОК)

Spatially, Figure 3 reveals that cropland, initially the dominant land type, was gradually supplanted by grassland and construction land. Forest areas expanded significantly along northern and eastern boundaries, while urban expansion and mining operations intensified within the mining zones. These transformations underscore the complex interaction between ecological recovery (e.g., forest expansion) and industrial development (e.g., construction land growth).

In the Anshan-Benxi region of China, a fluctuating decline in cropland area was observed, peaking at 16.76 % (3306.46 km²) in 1990, then steadily declining to 15.05 % (2968.50 km²) by 2020 (Table 3, 4). Forests, while dominant, showed a declining trend from 40.44 % (7978.63 km²) in 1985 to 36.73 % (7246.15 km²) in 2020. Grassland initially declined from 38.71 % to 35.18 % by 2000, later stabilizing at 34.13 % (6733.02 km²) in 2020. Wetland recovery was consistent, with wetland area expanding from 0.02 % (4.07 km²) in 1985 to 0.54 % (106.21 km²) in 2020. Water body areas remained stable, peaking at 234.40 km² (1.19 %) in 2005, and showing slight decreases. The share of construction land increased more than twofold, from 5.62 % (1108.63 km²) in 1985 to 12.51 % (2468.95 km²) by 2020.

As shown in Figure 4, cropland, initially prominent around the mining periphery, was gradually replaced by grassland and construction land. Forest and grassland coverage fluctuated, primarily in the northern and eastern zones, while urbanization intensified within and around the mining areas. The wetland recovery was evident, and water body areas remained stable.

Table 3
Таблица 3

LULC area (km^2) and proportion (%) of LGOK and SGOK iron ore affected areas in Russia, 1985–2020
Площадь (км^2) и доля (%)землепользования / наземного покрова зоны воздействия железорудного производства ЛГОК и СГОК в России с 1985 по 2020 год

Time	LULC area	Cropland	Forest	Grassland	Wetland	Water body	Bareland	Construction land
1985	Area	4264.68	1016.40	2314.98	4.45	92.90	0.00	317.70
	Proportion	53.23	12.69	28.90	0.06	1.16	0.00	3.97
1990	Area	4001.06	1022.81	2549.10	3.67	98.50	0.00	335.97
	Proportion	49.94	12.77	31.82	0.05	1.23	0.00	4.19
1995	Area	4005.88	990.86	2561.45	3.60	90.72	0.00	358.60
	Proportion	50.00	12.37	31.97	0.04	1.13	0.00	4.48
2000	Area	3776.91	1362.81	2392.83	7.83	95.90	0.03	374.80
	Proportion	47.15	17.01	29.87	0.10	1.20	0.00	4.68
2005	Area	3722.14	1363.03	2401.56	7.98	98.21	0.03	418.15
	Proportion	46.46	17.01	29.98	0.10	1.23	0.00	5.22
2010	Area	3696.26	1357.14	2401.22	8.13	99.68	0.03	448.65
	Proportion	46.14	16.94	29.97	0.10	1.24	0.00	5.60
2015	Area	3666.47	1335.30	2404.95	8.40	101.88	0.03	494.07
	Proportion	45.77	16.67	30.02	0.10	1.27	0.00	6.17
2020	Area	3623.90	1337.35	2407.55	8.79	105.07	0.03	528.41
	Proportion	45.24	16.69	30.05	0.11	1.31	0.00	6.60

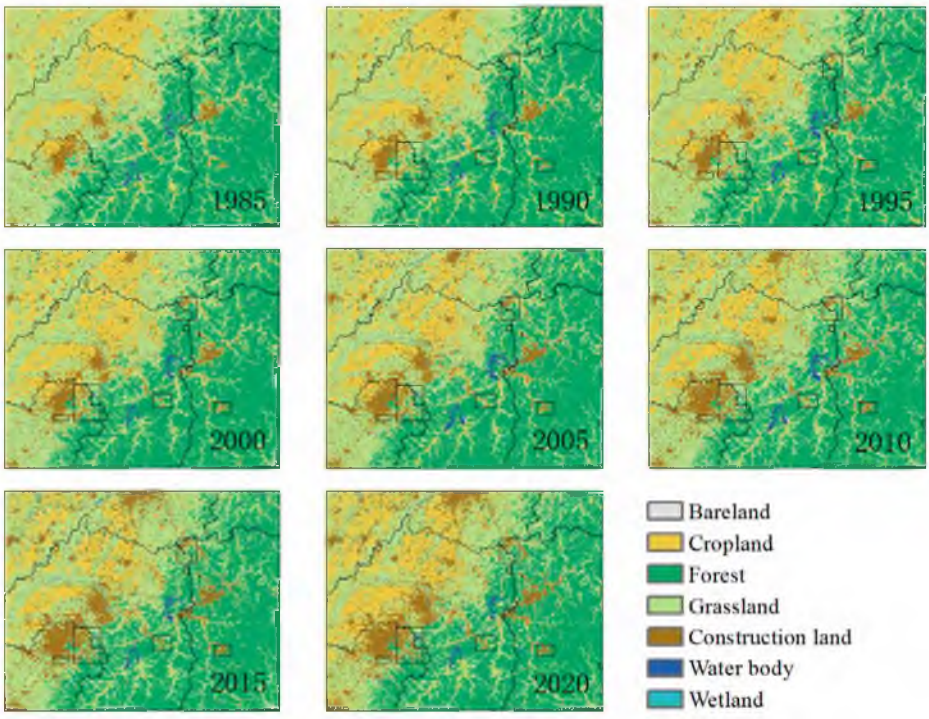

Fig. 4. LULC distribution map of the affected area of Anshan-Benxi Iron Ore Mine
Рис. 4. Карта распределения классов землепользования / наземного покрова в зоне воздействия рудника Аньшань-Бэньси

Table 4
Таблица 4

LULC area (km^2) and proportion (%) of Anshan-Benxi Iron ore affected area, 1985–2020
Площадь землепользования / наземного покрова (км^2) и доля (%)
от зоны воздействия рудника Аньшань-Бэньси в период с 1985 по 2020 год

Time	LULC area	Cropland	Forest	Grassland	Wetland	Water body	Bareland	Construction land
1985	Area	2855.80	7978.63	7637.40	4.07	145.11	0.36	1108.63
	Proportion	14.47	40.44	38.71	0.02	0.74	0.00	5.62
1990	Area	3306.46	7951.74	7125.62	3.74	157.35	1.46	1183.62
	Proportion	16.76	40.30	36.12	0.02	0.80	0.01	6.00
1995	Area	3072.89	7576.56	7564.49	14.29	207.40	1.80	1429.89
	Proportion	15.57	38.40	38.34	0.07	1.05	0.01	7.25
2000	Area	3153.34	7960.77	6941.95	54.55	188.78	0.73	1429.89
	Proportion	15.98	40.35	35.18	0.28	0.96	0.00	7.25
2005	Area	2706.98	7699.82	7283.61	68.88	234.40	0.37	1735.93
	Proportion	13.72	39.03	36.92	0.35	1.19	0.00	8.80
2010	Area	2390.25	7052.82	7865.91	91.57	233.34	1.29	2094.82
	Proportion	12.11	35.75	39.87	0.46	1.18	0.01	10.62
2015	Area	2253.69	7221.69	7516.94	179.03	213.79	3.79	2340.96
	Proportion	11.42	36.60	38.10	0.91	1.08	0.02	11.86
2020	Area	2968.50	7246.15	6733.02	106.21	204.40	2.76	2468.95
	Proportion	15.05	36.73	34.13	0.54	1.04	0.01	12.51

Overall, LULC changes from 1985 to 2020 in the LGOK and SGOK regions in Russia and the Anshan-Benxi regions in China illustrate the diverse impacts of mining, urbanization, and ecological initiatives. Common patterns across both regions include reductions in cropland, expansions of construction land, and some degree of wetland recovery, highlighting the influence of mining activities on LULC changes [Liu et al., 2023; Rasskazov et al., 2023]. However, regional differences emerge: forest recovery was more pronounced in Russia, potentially due to less intensive urbanization [Kou et al., 2014], while construction land expansion was more dominant in China, likely driven by extensive urban and industrial development [Hu et al., 2024]. Wetland recovery and water body stability were observed in both regions, while bareland remained a minimal fraction.

LULC dynamic analysis

Table 5 presents the changes in the proportion of vegetation cover and bareland + construction land in the affected areas of the LGOK and SGOK iron ore regions in Russia and the Anshan-Benxi iron ore region in China from 1985 to 2020. These changes reflect the varying impacts of mining development, urbanization, and ecological processes on land use in the two regions.

In the LGOK and SGOK regions, vegetation cover decreased gradually, from 94.87 % in 1985 to 92.09 % in 2020. Concurrently, the proportion of bareland + construction land rose from 3.97 % to 6.60 %. This steady decline in vegetation cover suggests the combined influence of mining development and infrastructure expansion, which resulted in the conversion of vegetated areas to construction land. The relatively moderate rate of vegetation loss may also reflect efforts to mitigate ecological impacts, such as natural vegetation regeneration or policy-driven restoration initiatives.

Table 5
Таблица 5

Proportion (%) of Vegetation and Bareland + Construction land in LGOK and SGOK and Anshan-Benxi iron ore affected areas from 1985 to 2020
Процентное соотношение (%) растительности и незастроенной территории плюс земли для строительства в зонах воздействия месторождений железной руды ЛГОКа и СГОКа и районе Аншань-Бэньси с 1985 по 2020 год

Time	LGOK and SGOK		Anshan-Benxi	
	Vegetation	Bareland+ Construction land	Vegetation	Bareland+ Construction land
1985	94.87	3.97	93.64	5.62
1990	94.58	4.19	93.20	6.01
1995	94.39	4.48	92.39	7.26
2000	94.12	4.68	91.79	7.25
2005	93.55	5.22	90.01	8.80
2010	93.15	5.60	88.19	10.62
2015	92.56	6.17	87.03	11.88
2020	92.09	6.60	86.44	12.53

In contrast, the Anshan-Benxi region experienced a more pronounced decline in vegetation cover, dropping from 93.64 % in 1985 to 86.44 % in 2020, coupled with a significant increase in bareland + construction land, which rose from 5.62 % to 12.53 %. This sharper decline in vegetation and rapid expansion of construction land likely reflects the more intensive mining activities and urbanization pressures in this region. The Anshan-Benxi region's proximity to densely populated urban areas and its role as an industrial hub may have amplified the extent of land-use changes, with mining-related developments exerting a stronger impact on the local environment.

The analysis of LULC changes in the LGOK and SGOK mining areas from 1985 to 2020 reveals significant dynamic transitions and conversion patterns among different land use types (Fig. 5 and 6, Tables 6 and 7).

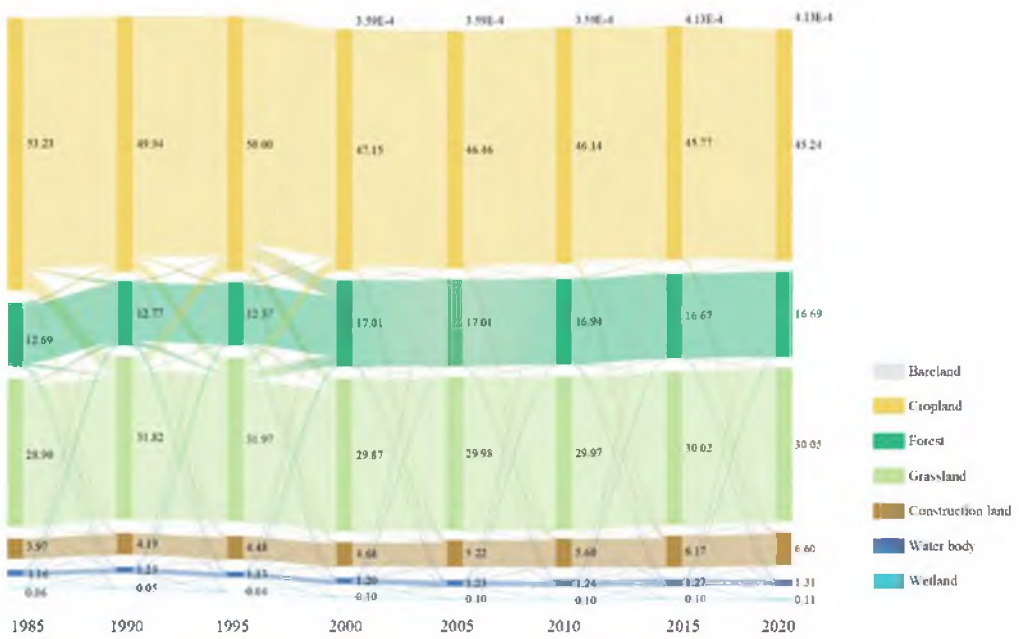

Fig. 5. Sankey diagram of LULC changes in the affected area of LGOK and SGOK Iron Ore Mine
Рис. 5. Диаграмма Сэнкей по изменению классов землепользования / наземного покрова в зоне воздействия рудников ЛГОК и СГОК

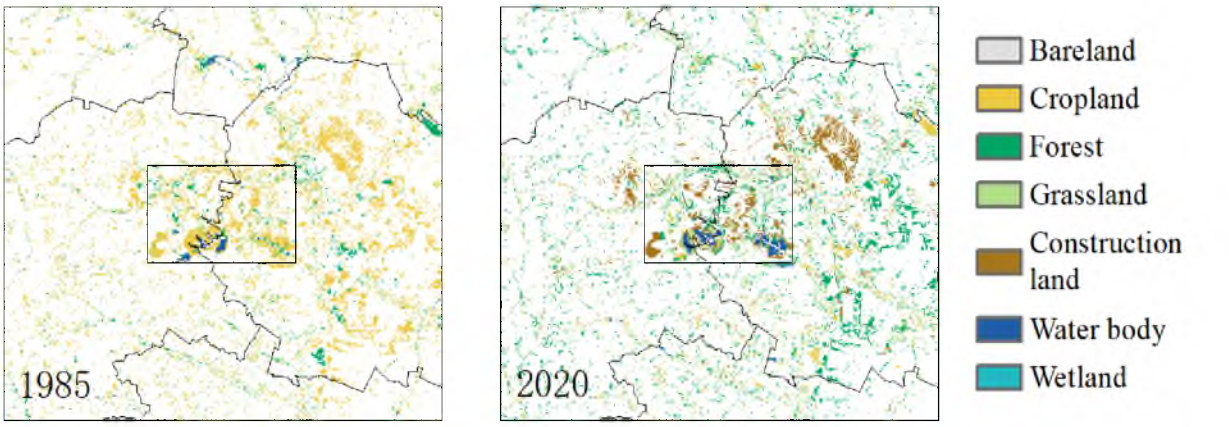

Fig. 6. LULC change map of the affected area of LGOK and SGOK Iron Ore Mines in Russia
Рис. 6. Карта изменений LULC в зоне воздействия рудников ЛГОК и СГОК в России

Table 6
Таблица 6

LULC area change (km^2) and change rate (%) in the affected area of LGOK and SGOK Iron Ore Mines
Изменение площади землепользования / наземного покрова (км^2) и скорость изменений (%) в зоне воздействия рудников ЛГОК и СГОК

Time	Changes	Cropland	Forest	Grassland	Wetland	Water body	Bareland	Construction land	S[1]
1985–1990	Area change	–263.62	6.41	234.12	–0.77	5.60	0.00	18.27	0.16
	Change rate	–0.01	0.00	0.02	–0.03	0.01	—	0.01	
1990–1995	Area change	4.82	–31.95	12.35	–0.07	–7.78	0.00	22.63	0.16
	Change rate	0.00	–0.01	0.00	–0.00	–0.02	—	0.01	
1995–2000	Area change	–228.97	371.95	–168.63	4.23	5.19	0.03	16.20	0.13
	Change rate	–0.01	0.08	–0.01	0.23	0.01	—	0.01	
2000–2005	Area change	–54.77	0.21	8.73	0.16	2.31	0.00	43.36	0.01
	Change rate	–0.00	0.00	0.00	0.00	0.00	0.00	0.02	
2005–2010	Area change	–25.88	–5.88	–0.34	0.14	1.47	0.00	30.50	0.01
	Change rate	–0.00	–0.00	–0.00	0.00	0.00	0.00	0.01	
2010–2015	Area change	–29.79	–21.84	3.74	0.27	2.20	0.00	45.42	0.01
	Change rate	–0.00	–0.00	0.00	0.01	0.00	0.03	0.02	
2015–2020	Area change	–42.57	2.05	2.60	0.39	3.18	0.00	34.34	0.01
	Change rate	–0.00	0.00	0.00	0.01	0.01	0.00	0.01	
1985–2020	Area change	–640.78	320.95	92.58	4.34	12.17	0.03	210.72	0.02
	Change rate	–0.00	0.01	0.00	0.03	0.00	—	0.02	

[1] S represents comprehensive land-use dynamics.

Table 7
Таблица 7

Matrix of LULC change and transfer (km^2) in the affected area of LGOK and SGOK Iron Ore Mine in Russia from 1985 to 2020
Матрица изменений и трансформаций классов землепользования / наземного покрова (км^2) в зоне воздействия железорудного производства ЛГОК и СГОК в России с 1985 по 2020 год

LULC type	Cropland	Forest	Grassland	Wetland	Water body	Bareland	Construction land
Cropland	0	23	0	0	0	0	0
Forest	0	2424574	39630	54122	0	2495	26
Grassland	0	235447	621005	68293	0	5200	337
Wetland	0	164509	34932	1472251	1	2918	123
Water body	0	125307	6369	12495	220994	2402	5
Bareland	0	15019	5090	2408	0	50443	126
Construction land	0	1705	0	768	0	1164	2477

Overall, bareland exhibited the smallest degree of change, maintaining relative stability throughout the study period. Grassland and cropland experienced moderate fluctuations, while wetland and construction land showed the largest changes. Construction land consistently increased, reflecting regional development and urban expansion, while cropland area decreased significantly, indicating land conversion driven by mining and infrastructure growth. Among the seven land use types, all except cropland showed an overall increase in area.

The comprehensive land-use dynamics index (S) peaked during 1985–1995, indicating that this was the most intense period of LULC change. After 2000, the S value stabilized at 0.01, suggesting a trend toward land-use equilibrium, possibly driven by a balance between development activities and ecological restoration efforts.

The Sankey diagram (Figure 5) and transfer matrix (Table 7) provide further insights into land-use conversion patterns.

Cropland Decline: Cropland was the primary donor land type, transitioning into forest, grassland, and construction land. Between 1995 and 2000, 251.87 km^2 of cropland was converted to forest. Significant cropland-to-grassland conversions were observed during 1985–2000, with conversion areas of 283.65, 174.90, and 163.66 km^2, respectively. However, between 1990 and 2000, grassland-to-cropland conversions exceeded cropland-to-grassland transitions. After 2000, cropland-to-grassland conversions declined sharply.

Construction Land Expansion: Construction land primarily expanded through cropland conversions, with the largest conversion (41.16 km^2) occurring between 2010 and 2015, reflecting infrastructure and urban development demands.

Forest and Wetland Recovery: Grassland contributed significantly to forest increases, particularly between 1995 and 2000, when 167.80 km^2 of grassland was converted to forest. Wetland increases were primarily sourced from cropland, with the largest transfer of 9.81 km^2 occurring during 1995-2000, highlighting localized hydrological recovery.

The spatial distribution of LULC changes (Figure 6) reveals that 14.01% of the study area underwent significant transformations between 1985 and 2020. These changes were concentrated

within the mining cores and in the eastern portion of the study region, where mining and urbanization activities were most intense. Construction land expanded significantly, replacing cropland in the core and surrounding areas of the mines, reflecting the direct impact of mining operations and regional development. In contrast, forest areas exhibited slight increases in some regions, likely due to vegetation restoration efforts or the implementation of environmental protection policies.

The analysis of LULC changes in the Anshan-Benxi iron ore affected area from 1985 to 2020 highlights significant dynamic transitions and conversion patterns among different land use types (Figures 7 and 8; Tables 8 and 9).

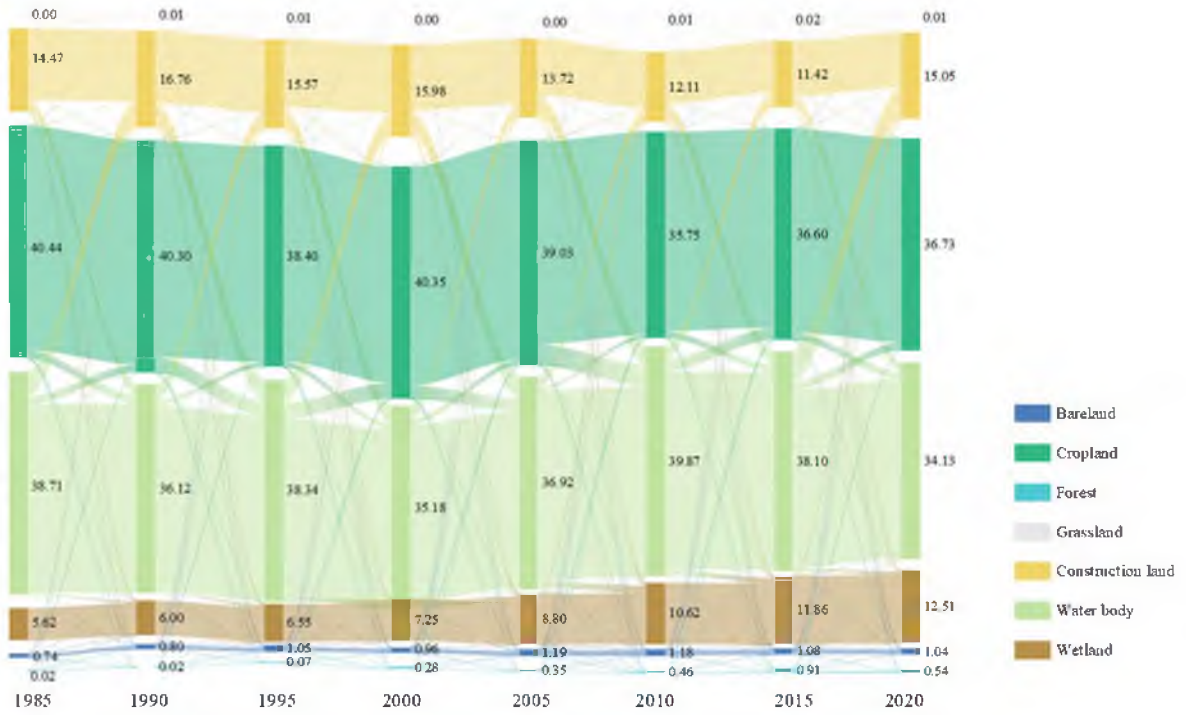

Fig. 7. Sankey diagram of LULC changes
in the affected area of Anshan-Benxi Iron Ore Mine in China
Рис. 7. Диаграмма Санкей по изменению классов землепользования / наземного покрова
в зоне воздействия железорудного производства Аньшан-Бэньси в Китае

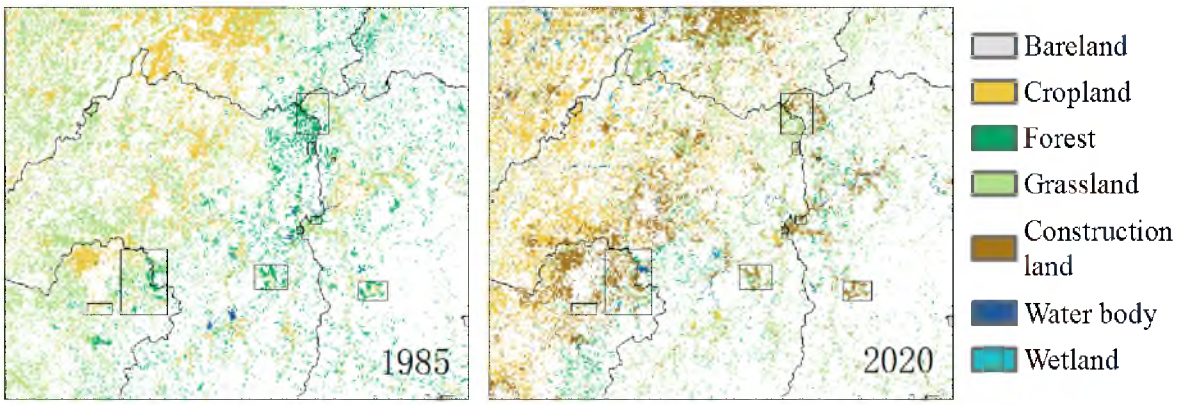

Fig. 8. LULC change map of the affected area
of Anshan-Benxi Iron Ore Mine in China
Рис. 8. Карта изменений землепользования / наземного покрова
в зоне воздействия рудника Аньшань-Бэньси в Китае

Table 8
Таблица 8

LULC area change (km^2) and change rate (%) in the affected area of Anshan-Benxi Iron Ore Mine
Изменение площади классов землепользования / наземного покрова (км^2)
и скорости изменений (%) в зоне воздействия рудника Аньшань-Бэньси

Time	Changes	Cropland	Forest	Grassland	Wetland	Water body	Bareland	Construction land	S[1]
1985–1990	Area change	450.66	–26.89	–511.78	–0.33	12.23	1.11	74.99	0.28
	Change rate	3.16	–0.07	–1.34	–1.61	1.69	62.36	1.35	
1990–1995	Area change	–233.57	–375.18	438.87	10.55	50.05	0.34	246.27	0.33
	Change rate	–1.41	–0.94	1.23	56.44	6.36	4.63	1.84	
1995–2000	Area change	80.44	384.21	–622.54	40.26	–18.62	–1.07	0.00	0.45
	Change rate	0.52	1.01	–1.65	56.35	–1.80	–11.90	2.12	
2000–2005	Area change	–446.35	–260.95	341.66	14.34	45.62	–0.36	306.04	0.43
	Change rate	–2.83	–0.66	0.98	5.26	4.83	–9.74	4.28	
2005–2010	Area change	–316.74	–647.00	582.30	22.69	–1.06	0.91	358.89	0.42
	Change rate	–2.34	–1.68	1.60	6.59	–0.09	48.63	4.13	
2010–2015	Area change	–136.55	168.88	–348.98	87.46	–19.54	2.51	246.14	0.37
	Change rate	–1.14	0.48	–0.89	19.10	–1.68	38.99	2.35	
2015–2020	Area change	714.81	24.46	–783.91	–72.82	–9.40	–1.03	127.99	0.55
	Change rate	6.34	0.07	–2.09	–8.13	–0.88	–5.44	1.09	
1985–2020	Area change	112.70	–732.48	–904.38	102.14	59.28	2.41	1360.32	0.07
	Change rate	0.11	–0.26	–0.34	71.77	1.17	19.33	3.51	

[1] S represents Comprehensive land-use dynamics.

Table 9
Таблица 9

Matrix of LULC change and transfer (km^2) in the affected area of Anshan-Benxi Iron Ore Mine in China from 1985 to 2020
Матрица изменений и трансформаций классов землепользования / наземного покрова (км^2)
в зоне воздействия железорудного производства Аньшань-Бэньси в Китае с 1985 по 2020 год

LULC type	Cropland	Forest	Grassland	Wetland	Water body	Bareland	Construction land
Cropland	1557.90	18.93	1369.08	0.14	22.44	0.02	0.00
Forest	12.85	6946.87	285.31	0.01	1.11	0.00	0.00
Grassland	765.17	914.31	5035.94	0.20	17.20	0.20	0.00
Wetland	52.94	0.82	38.86	3.52	10.07	0.00	0.00
Water body	45.20	10.71	59.59	0.09	88.80	0.02	0.00
Bareland	0.72	0.91	1.08	0.00	0.05	0.01	0.00
Construction land	421.03	86.09	847.54	0.11	5.45	0.10	1108.63

Over the study period, forest exhibited the smallest degree of change, reflecting relative stability. Grassland and cropland followed with moderate fluctuations, while wetland and bareland experienced the most significant changes. Construction land showed a consistent increase across all periods, aligning with drivers of industrial and urban development. Among the

land-use types, all except forest and grassland exhibited an overall increase in area, reflecting a shift toward more anthropogenic land uses.

The comprehensive land-use dynamics index (S) peaked at 0.55 during 2015–2020, indicating the most intense LULC changes during this period. The lowest value of S (0.01) was recorded during 1985–1990, suggesting relative land-use stability. The overall trend in S showed an increase from 1985–2000, a decrease from 2000–2015, and a subsequent increase during 2015–2020, highlighting varying pressures on land use over time.

The Sankey diagram (Figure 7) and transfer matrix (Table 9) further reveal key land conversion patterns:

Grassland Reduction and Cropland Increase: Grassland-to-cropland conversions were the largest source of cropland growth, particularly during 2015–2020, when 1040.01 km² of grassland was converted. This accounted for a significant portion of grassland reduction.

Grassland Conversion to Construction Land: Grassland also contributed substantially to the expansion of construction land, especially during 2005–2010, when 245.93 km² of grassland was converted.

Forest Reduction: Forest loss was primarily driven by its conversion to grassland, with the highest conversion observed during 2005–2010, totaling 714.52 km².

Wetland and Water Body Increases: Wetland and water body areas increased, primarily sourced from cropland and grassland conversions. For example, during 2010–2015, 77.88 km² of cropland and 42.34 km² of grassland were converted into wetland. Similarly, from 1990-1995, cropland and grassland transfers to water bodies reached 31.83 km² and 30.31 km², respectively.

The spatial distribution of LULC changes (Figure 8) reveals that approximately 25.28 % of the study area underwent significant transformations between 1985 and 2020. Changes were concentrated in the northwestern region, influenced by topography and urban expansion, while fewer changes were observed in the southeastern areas. Construction land expanded significantly near the mining areas and the provincial capital, Shenyang. This expansion was driven by the conversion of grassland and forest near mining sites and cropland in the northern region, reflecting the pressures of urban and industrial development. In contrast, grassland and cropland exhibited notable decreases, largely attributed to mining activities and urban growth in proximity to the mining areas. Forest areas increased slightly in localized regions, particularly along the boundary between Liaoyang and Anshan.

The establishment of changes in land cover has important practical applications for substantiating the boundaries of sanitary protection zones in the context of the prospective development of the mining industry [Полетаев, Лисецкий, 2023]. The LULC changes observed in both the LGOK and SGOK regions in Russia and the Anshan-Benxi region in China highlight the complex interplay between industrial development, urbanization, and ecological recovery [Lambin et al., 2003]. While construction land expansion was a common feature driven by mining and urban growth, significant regional differences in land-use dynamics and ecological impacts underscore the importance of tailored land management strategies.

In the LGOK and SGOK regions, the modest percentage of changed areas (14.01 %) and the observed recovery of forest and wetland areas suggest relatively effective land management practices [Galperin, 2015]. The stabilization of the S index after 2000 indicates a balance between development and ecological restoration, reflecting some degree of success in mitigating the environmental impacts of mining [Chazdon, 2008]. However, the continued decline in cropland highlights the need for strategies that support economic growth while minimizing agricultural land losses.

Conversely, the Anshan-Benxi region experienced more intense land-use changes, with 25.28 % of the area undergoing significant transformations [Liu et al., 2023]. The pronounced reduction in grassland and cropland, coupled with the rapid expansion of construction land, reflects greater pressure from industrialization and urbanization [Seto et al., 2012]. The Anshan-Benxi region's proximity to densely populated urban areas and its role as an industrial hub have

amplified the extent of land-use changes, with mining-related developments exerting a stronger impact on the local environment [Kou et al., 2024]. While localized forest and wetland recovery efforts have shown promise [Wu et al., 2024], the overall shift from ecological to anthropogenic land use has disrupted the regional ecosystem balance.

These findings emphasize the urgent need for integrated policies that balance economic growth with environmental conservation, such as soil improvement measures [Kong et al., 2023], stricter land-use regulations, and enhanced ecological restoration initiatives. Collectively, these findings underscore the critical role of adaptive and region-specific land management strategies in mining regions [Turner et al., 1995].

For the LGOK and SGOK regions, continued emphasis on ecological restoration and sustainable practices will be essential to maintain the current balance between development and environmental protection [Chazdon, 2008]. In the Anshan-Benxi region, additional efforts are required to curb the rapid loss of natural land uses, ensure sustainable urban expansion, and mitigate the ecological impacts of mining activities [Worlanyo, Jiangfeng, 2021].

Estimation of carbon sequestration

As shown in Figure 9, from 1985 to 2020, the total carbon sink (sum of all types) in the Russian iron mining areas remained generally stable, with a slight increase from 102.3 Mt to 106.0 Mt. Specifically, the carbon sink capacity of forest and grassland areas remained relatively stable, while that of cropland experienced a slight decline. Forest carbon sequestration decreased to 27.2 Mt in 1995 but subsequently recovered, reaching a peak of 37.5 Mt in 2000. Grassland carbon sequestration showed fluctuations, gradually declining after 1995. Cropland carbon sequestration demonstrated minor variations over the time periods but showed a slight overall decrease. In terms of period-specific changes, forest carbon sequestration increased substantially between 1995 and 2000 (+10.23 Mt), while that of grassland and cropland decreased by 2.31 Mt and 2.29 Mt, respectively. Overall, the changes in carbon sequestration in the Russian iron mining areas were minimal during the study period, with total carbon sequestration increasing by only 3.69 Mt.

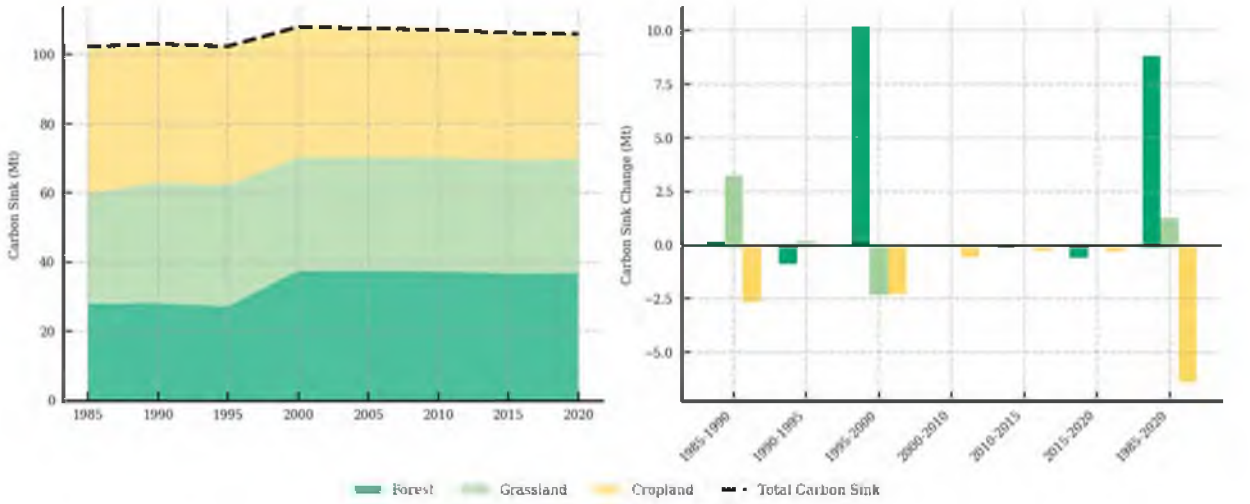

Fig. 9. Carbon Sequestration in the Affected Area of LGOK and SGOK Iron Ore Mines
Рис. 9. Поглощение углерода в зоне воздействия железорудных месторождений ЛГОК и СГОК

In contrast, as illustrated in Figure 10, the carbon sequestration in the Chinese iron mining areas showed a significant declining trend from 1985 to 2020, decreasing from 352.6 Mt to 321.2 Mt. Forest carbon sink capacity decreased most notably, especially between 2010 and 2015, with a reduction of 17.79 Mt. Grassland carbon sequestration fluctuated significantly over the study period, with an increase between 1990 and 1995, followed by substantial variations.

Cropland carbon sequestration, meanwhile, showed an overall decline after 1990, particularly between 2000 and 2010. Regarding changes across various periods, forest carbon sequestration decreased by 20.14 Mt, that of grassland fell by 12.39 Mt, and cropland sequestration reduced by 1.13 Mt between 1985 and 2020. The total carbon sequestration in the Chinese iron mining areas declined by 31.41 Mt over the study period, indicating a notable downward trend.

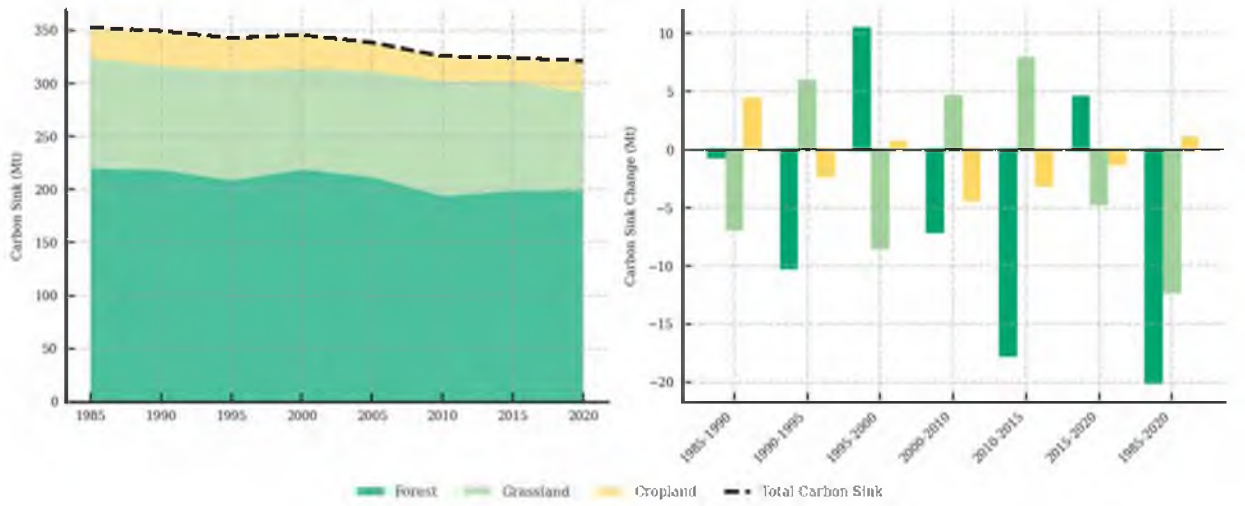

Fig. 10. Carbon Sequestration in the Affected Area of Anshan-Benxi Iron Ore Mine
Рис. 10. Секвестрация углерода в зоне воздействия рудника Аньшань-Бэньси

In summary, during the study period, the total carbon sequestration in the Russian iron mining areas remained stable, with a slight increase of 3.69 Mt, while the Chinese iron mining areas experienced a significant decrease of 31.41 Mt, primarily due to reductions in forest and grassland carbon sink capacity. These findings further underscore the necessity of strengthening environmental protection and sustainable practices in the Chinese mining areas to mitigate the adverse impacts of land-use changes on carbon sequestration and regional ecosystems [Han, Li, 2022].

Conclusion

This study provides a comprehensive analysis of LULC dynamics and changes in carbon sequestration in the LGOK and SGOK iron ore regions in Russia and the Anshan-Benxi iron ore region in China from 1985 to 2020. The findings reveal that mining activities and urban expansion significantly influenced LULC patterns and carbon sequestration capacity in both regions, though with differing degrees and trends.

In Russia, cropland area decreased by approximately 8 % (640.78 km²), primarily replaced by construction land and forest. Forest cover increased from 12.69 % to 16.69 %, reflecting effective ecological management practices. Consequently, the total carbon sequestration in Russian mining regions remained stable, with a slight increase of 3.69 Mt over the study period. In contrast, the Anshan-Benxi region in China experienced stronger development pressures, leading to a decrease in forest cover from 40.44 % to 36.73 % and an increase in construction land from 5.62 % to 12.51 %. These changes contributed to a significant decline in total carbon sequestration by 31.41 Mt, driven largely by reductions in forest and grassland carbon sink capacity.

These contrasting trends underscore the importance of sustainable land management strategies that prioritize ecological restoration alongside industrial growth. Effective strategies such as afforestation, wetland restoration, and adaptive land-use policies are critical for mitigating the environmental impacts of mining and maintaining carbon sequestration capacities. Future policies should focus on harmonizing economic growth with environmental conservation, ensuring that industrial development in mining regions is balanced with sustainable land use to promote long-term ecological and economic stability.

Список литературы

Беленко В.В., Ассех К.Ф. 2022. Проблемные вопросы обнаружения изменений состава земель методами дистанционного зондирования Земли из космоса для целей рационального использования на примере Республики Кот-д'Ивуар. Известия высших учебных заведений. Геодезия и аэрофотосъемка, 66(4): 86–100. https://doi.org/10.30533/0536-101X-2022-66-4-86-100.

Гзогян С.Р., Гзогян Т.Н. 2018. Особенности вещественного состава богатых железных руд месторождений КМА. Научные ведомости Белгородского государственного университета. Серия: Естественные науки, 42(2): 131–141. https://doi.org/10.18413/2075-4671-2018-42-2-131-141.

Кирсанов А.К. 2023. Обзор современного состояния горнодобывающей промышленности Китая. Горные науки и технологии, 8(2): 115–127. https://doi.org/10.17073/2500-0632-2022-11-35.

Корнилов А.Г., Кичигин Е.В., Колмыков С.Н., Новых Л.Л., Дроздова Е.А., Петин А.Н., Присный А.В., Лазарев А.В., Колчанов А.Ф. 2015. Экологическая ситуация в районах размещения горнодобывающих предприятий региона Курской магнитной аномалии. Белгород, Изд. Белгородского государственного университета, 157 с.

Полетаев А.О., Лисецкий Ф.Н. 2023. Использование мониторинговых данных и ГИС-технологий для корректировки границ санитарно-защитных зон в связи с развитием Старооскольско-Губкинского промышленного района. Геополитика и экогеодинамика регионов, 9(3): 338–347.

Савин И.Ю., Березуцкая Э.Р. 2024. Концепция наземного покрова (Land Cover) как основа дистанционного мониторинга земель. Региональные геосистемы, 48(1): 77–90. https://doi.org/10.52575/2712-7443-2024-48-1-77-90.

Хуан Л., Полетаев А.О. 2024. Использование возможностей космического мониторинга для выявления особенностей трансформации земель в зоне влияния ведущих железорудных предприятий России и Китая. В кн.: Геоэкология и рациональное недропользование: от науки к практике. Материалы IV Всероссийской научной конференции молодых ученых, Белгород, 10 октября 2024. Белгород, Белгородский государственный национальный исследовательский университет: 117–125.

Abbas Z., Yang G., Zhong Y., Zhao Y. 2021. Spatiotemporal Change Analysis and Future Scenario of LULC Using the CA-ANN Approach: A Case Study of the Greater Bay Area, China. Land, 10(6): 584. https://doi.org/10.3390/land10060584.

Alshari E.A., Gawali B.W. 2021. Development of a Classification System for LULC Using Remote Sensing and GIS. Global Transitions Proceedings, 2(1): 8–17. https://doi.org/10.1016/j.gltp.2021.01.002.

Anderson J.R. 1976. A Land Use and Land Cover Classification System for Use with Remote Sensor Data. US Government Printing Office, 28 p.

Basheer S., Wang X., Farooque A.A., Nawaz R.A., Liu K., Adekanmbi T., Liu S. 2022. Comparison of Land Use Land Cover Classifiers Using Different Satellite Imagery and Machine Learning Techniques. Remote Sensing, 14(19): 4978. https://doi.org/10.3390/rs14194978.

Chazdon R.L. 2008. Beyond Deforestation: Restoring Forests and Ecosystem Services on Degraded Lands. Science, 320(5882): 1458–1460. https://doi.org/10.1126/science.1155365.

Di Gregorio A. 2005. Land Cover Classification System: Classification Concepts and User Manual. Rome, Food and Agriculture Organization of the United Nations, 208 p.

Digra M., Dhir R., Sharma N. 2022. Land Use Land Cover Classification of Remote Sensing Images Based on the Deep Learning Approaches: A Statistical Analysis and Review. Arabian Journal of Geosciences, 15: 1003. https://doi.org/10.1007/s12517-022-10246-8.

Foley J.A., Defries R., Asner G.P., Barford C., Bonan G., Carpenter S.R., Chapin F.S., Coe M.T., Daily G.C., Gibbs H.K., Helkowski J.H., Holloway T., Howard E.A., Kucharik Ch.J., Monfreda Ch., Patz J.A., Prentice I.C., Ramankutty N., Snyder P.K. 2005. Global Consequences of Land Use. Science, 309(5734): 570–574. https://doi.org/10.1126/science.1111772.

Galperin A. 2015. Using of Man-Made Massives in Russian Mining (Engineering: Geological Aspects). Engineering Geology for Society and Territory, 6: 1057–1062. https://doi.org/10.1007/978-3-319-09060-3_192.

Grimm N.B., Faeth S.H., Golubiewski N.E., Redman C.L., Wu J., Bai X., Briggs J.M. 2008. Global Change and the Ecology of Cities. Science, 319(5864): 756–760. https://doi.org/10.1126/science.1150195.

Han H., Li X. 2022. Sustainable Land Use Management in Mining Areas: Challenges and Strategies. Resources Policy, 76: 102616. https://doi.org/10.1016/j.resourpol.2022.102616.

Hu X., Liao W., Wei Y., Wei Z., Huang Sh. 2024. Analysis of Land Use Change and Its Economic and Ecological Value under the Optimal Scenario and Green Development Advancement Policy: A Case Study of Hechi, China. Sustainability, 16(12): 5039. https://doi.org/10.3390/su16125039.

Kou X., Zhao J., Sang W. 2024. Impact of Typical Land Use Expansion Induced by Ecological Restoration and Protection Projects on Landscape Patterns. Land, 13(9): 1513. https://doi.org/10.3390/land13091513.

Lal R. 2004. Soil Carbon Sequestration Impacts on Global Climate Change and Food Security. Science, 304(5677): 1623–1627. https://doi.org/10.1126/science.1097396.

Lambin E.F., Geist H.J. 2008. Land-Use and Land-Cover Change: Local Processes and Global Impacts. Springer Science & Business Media, 222 p.

Lambin E.F., Geist H.J., Lepers E. 2003. Dynamics of Land-Use and Land-Cover Change in Tropical Regions. Annual Review of Environment and Resources, 28(1): 205–241. https://doi.org/10.1146/annurev.energy.28.050302.105459.

Liu H., Wang Q., Liu N., Zhang H., Tan Y., Zhang Z. 2023. The Impact of Land Use/Cover Change on Ecological Environment Quality and Its Spatial Spillover Effect under the Coupling Effect of Urban Expansion and Open-Pit Mining Activities. Sustainability, 15(20): 14900. https://doi.org/10.3390/su152014900.

Liu Y., Li J., Yang Y. 2023. Urbanization and Its Effects on Land Use and Land Cover Change in the Anshan-Benxi Region, China. Journal of Geographical Sciences, 33(2): 245–260. https://doi.org/10.1007/s11442-023-2035-6.

Liu Y., Zhan J., Deng X. 2005. Spatio-Temporal Patterns and Driving Forces of Urban Land Expansion in China During the Economic Reform Era. Ambio: A Journal of the Human Environment, 34(6): 450–455. https://doi.org/10.1579/0044-7447-34.6.450.

Ni J. 2013. Carbon Storage in Chinese Terrestrial Ecosystems: Approaching a More Accurate Estimate. Climatic Change, 119(3): 905–917. https://doi.org/10.1007/s10584-013-0767-7.

Pan Y., Birdsey R.A., Fang J., Houghton R., Kauppi P.E., Kurz W.A., Phillips O.L., Shvidenko A., Lewis S.L., Canadell J.G., Ciais P., Jackson R.B., Pacala S.W., McGuire A.D., Piao S., Rautiainen A., Sitch S., Hayes D. 2011. A Large and Persistent Carbon Sink in the World's Forests. Science, 333(6045): 988–993. https://doi.org/10.1126/science.1201609.

Pang Z., Bu J., Yuan Y., Zheng J., Xue Q., Wang J., Guo H., Zuo H. 2023. The Low-Carbon Production of Iron and Steel Industry Transition Process in China. Steel Research International, 95(3): 2300500. https://doi.org/10.1002/srin.202300500.

Pirnazar M., Haghighi N., Azhand D., Ostad-Ali-Askari K., Eslamian S., Dalezios N.R., Singh V.P. 2021. Land Use Change Detection and Prediction Using Markov-CA and Publishing on the Web with Platform Map Server: Case Study Qom Metropolis, Iran. Journal of Geography and Cartography, 4(1): 7–20. https://doi.org/10.24294/jgc.v4i1.453.

Pontius G.R., Malanson J. 2005. Comparison of the Structure and Accuracy of Two Land Change Models. International Journal of Geographical Information Science, 19(2): 243–265. https://doi.org/10.1080/13658810410001713434.

Post W.M., Kwon K.C. 2000. Soil Carbon Sequestration and Land-Use Change: Processes and Potential. Global Change Biology, 6(3): 317–327. https://doi.org/10.1046/j.1365-2486.2000.00308.x.

Seto K.C., Güneralp B., Hutyra L.R. 2012. Global Forecasts of Urban Expansion to 2030 and Direct Impacts on Biodiversity and Carbon Pools. Proceedings of the National Academy of Sciences, 109(40): 16083–16088. https://doi.org/10.1073/pnas.1211658109.

Turner B.L., Lambin E.F., Reenberg A. 2007. The Emergence of Land Change Science for Global Environmental Change and Sustainability. Proceedings of the National Academy of Sciences, 104(52): 20666–20671. https://doi.org/10.1073/pnas.0704119104.

Turner B.L., Skole D., Sanderson S., Fischer G., Fresco L., Leemans R. 1995. Land-Use and Land-Cover Change: Science/Research Plan. IGBP Report, 35: 132.

Verburg P.H., Schot P.P., Dijst M.J., Veldkamp A. 2004. Land Use Change Modelling: Current Practice and Research Priorities. GeoJournal, 61(4): 309–324. https://doi.org/10.1007/s10708-004-4946-y.

Wohlfart C., Mack B., Liu G., Kuenzer C. 2017. Multi-Faceted Land Cover and Land Use Change Analyses in the Yellow River Basin Based on Dense Landsat Time Series: Exemplary Analysis in Mining, Agriculture, Forest, and Urban Areas. Applied Geography, 85: 73–88. https://doi.org/10.1016/j.apgeog.2017.06.004.

Worlanyo A.S., Jiangfeng L. 2021. Evaluating the Environmental and Economic Impact of Mining for Post-Mined Land Restoration and Land-Use: A Review. Journal of Environmental Management, 279: 111623. https://doi.org/10.1016/j.jenvman.2020.111623.

Wu J., Yang J., Ma L., Li Z., Shen X. 2016. A System Analysis of the Development Strategy of Iron Ore in China. Resources Policy, 48: 32–40. https://doi.org/10.1016/j.resourpol.2016.01.010.

Wu Q., Wang L., Wang T., Chen H., Du P. 2024. Global Versus Local? A Study on the Synergistic Relationship of Ecosystem Service Trade-Offs from Multiple Perspectives Based on Ecological Restoration Zoning of National Land Space – A Case Study of Liaoning Province. Applied Sciences, 14(22): 10421. https://doi.org/10.3390/app142210421.

Xu Y., Li J., Zhang C., Raval S., Guo L., Yang F. 2024. Dynamics of Carbon Sequestration in Vegetation Affected by Large-Scale Surface Coal Mining and Subsequent Restoration. Scientific Reports, 14: 13479. https://doi.org/10.1038/s41598-024-64381-1.

Yifter T., Razoumny Yu., Lobanov V. 2022. Deep Transfer Learning of Satellite Imagery for Land Use and Land Cover Classification. Informatics and Automation, 21(5): 963–982. https://doi.org/10.15622/ia.21.5.5.

Zhang X., Liu L., Chen X., Gao Y., Xie S., Mi J. 2021. GLC_FCS30: Global Land Cover Product with Fine Classification System at 30 m Using Time-Series Landsat Imagery. Earth System Science Data, 13(6): 2753–2776. https://doi.org/10.5194/essd-13-2753-2021.

Zhang Z., Bai Z., He Z., Bao N. 2012. Dynamic Changes of Land Use Type and Carbon Sinks Based RS and GIS in Pingshuo Opencast Coal Mine. Transactions of the Chinese Society of Agricultural Engineering (Transactions of the CSAE), 28(3): 230–236. https://doi.org/10.3969/j.issn.1002-6819.2012.03.040.

Zheng L., Li Y., Chen Y., Wang R., Yan S., Xia C., Zhang B., Shao J. 2024. Driving Model of Land Use Change on the Evolution of Carbon Stock: A Case Study of Chongqing, China. Environmental Science and Pollution Research International, 31(3): 4238–4255. https://doi.org/10.1007/s11356-023-31335-5.

Kong T., Zhang K., Huang L., Di J., Wang Y., Zhang J. 2023. Effects of mixed application of microbial agents on growth and substrate properties of alfalfa in coal gangue matrix with different particle sizes. Journal of China Coal Society, 48(S1): 241–251. https://doi.org/10.13225/j.cnki.jccs.2022.0615 (in Chinese).

Shvidenko A., Nilsson S. 2003. A Synthesis of the Impact of Russian Forests on the Global Carbon Budget for 1961–1998. Tellus B: Chemical and Physical Meteorology, 55(2): 391–415. https://doi.org/10.3402/tellusb.v55i2.16722.

Di Gregorio A., Jansen L.J.M. 2006. Land Cover Classification System (LCCS): Classification Concepts and User Manual. Rome, FAO, 179 p.

Shelestov A., Lavreniuk M., Kussul N., Novikov A., Skakun S. 2017. Exploring Google Earth Engine Platform for Big Data Processing: Classification of Multi-Temporal Satellite Imagery for Crop Mapping. Frontiers in Earth Science, 5: 1–10. https://doi.org/10.3389/FEART.2017.00017.

Rasskazov I.Y., Arkhipova Y.A., Kryukov V.G., Volkov A.F. 2023. Mining Industry in the Russian Far East: Balancing the Interests of Subsoil Use and the State. Journal of Mining Science, 59(3): 481–489.

Rengma N.S., Yadav M. 2024. Generation and Classification of Patch-Based Land Use and Land Cover Dataset in Diverse Indian Landscapes: A Comparative Study of Machine Learning and Deep Learning Models. Environmental Monitoring and Assessment, 196(6): 568. https://doi.org/10.1007/s10661-024-12719-7.

Ahialey E.K., Kabo-Bah A.T., Gyamfi S. 2024. LULC Changes in the Region of the Proposed Pwalugu Hydropower Project Using GIS and Remote Sensing Technique. Journal of Geography and Cartography, 7(2): 8282. https://doi.org/10.24294/jgc.v7i2.8282.

References

Belenko V.V., Assekh K.F. 2022. Problematic Issues of Detecting Changes in Land Composition Using Remote Sensing Methods for Rational Land Use: The Case of Côte d'Ivoire. Annals of Higher Educational Institutions. Geodesy and Aerial Photography, 66(4): 86–100 (in Russian). https://doi.org/10.30533/0536-101X-2022-66-4-86-100.

Gzogyan S.R., Gzogyan T.N. 2018. Material Composition of Rich Iron Ore Deposits of KMA. Scientific Bulletin of Belgorod State University. Series: Natural Sciences, 42(2): 131–141 (in Russian). https://doi.org/10.18413/2075-4671-2018-42-2-131-141.

Kirsanov A.K. 2023. Chinese Mining Industry: State of the Art Review. Mining Science and Technology, 8(2): 115–127 (in Russian). https://doi.org/10.17073/2500-0632-2022-11-35.

Kornilov A.G., Kichigin E.V., Kolmykov S.N., Novykh L.L., Drozdova E.A., Petin A.N., Prisny A.V., Lazarev A.V., Kolchanov A.F. 2015. Environmental Situation in the Areas where Mining Enterprises on the Region of Kursk Magnetic Anomaly. Belgorod, Publ. Belgorod State University, 157 p. (in Russian).

Poletaev A.O., Lisetskiy F.N. 2023. The Use of Monitoring Data and GIS Technologies to Adjust the Boundaries of Sanitary Protection Zones in Connection with the Development of the Stary Oskol and Gubkin Industrial Area. Geopolitics and Ecogeodynamics of Regions, 9(3): 338–347 (in Russian).

Savin I.Yu., Berezutskaya E.R. 2024. The Concept of Land Cover as a Basis for Remote Sensing Monitoring of Land. Regional Geosystems, 48(1): 77–90 (in Russian). https://doi.org/10.52575/2712-7443-2024-48-1-77-90.

Huang L., Poletaev A.O. 2024. Using Space Monitoring Capabilities to Identify Land Transformation Features in the Influence Zones of Major Iron Ore Enterprises in Russia and China. In: Geoecology and Rational Subsoil Use: From Science to Practice. Proceedings of the 4th All-Russian Scientific Conference of Young Scientists, Belgorod, 10 October 2024. Belgorod, Pabl. Belgorod State National Research University: 117–125 (in Russian).

Abbas Z., Yang G., Zhong Y., Zhao Y. 2021. Spatiotemporal Change Analysis and Future Scenario of LULC Using the CA-ANN Approach: A Case Study of the Greater Bay Area, China. Land, 10(6): 584. https://doi.org/10.3390/land10060584.

Ahialey E.K., Kabo-Bah A.T., Gyamfi S. 2024. LULC Changes in the Region of the Proposed Pwalugu Hydropower Project Using GIS and Remote Sensing Technique. Journal of Geography and Cartography, 7(2): 8282. https://doi.org/10.24294/jgc.v7i2.8282.

Alshari E.A., Gawali B.W. 2021. Development of a Classification System for LULC Using Remote Sensing and GIS. Global Transitions Proceedings, 2(1): 8–17. https://doi.org/10.1016/j.gltp.2021.01.002.

Anderson J.R. 1976. A Land Use and Land Cover Classification System for Use with Remote Sensor Data. US Government Printing Office, 28 p.

Basheer S., Wang X., Farooque A.A., Nawaz R.A., Liu K., Adekanmbi T., Liu S. 2022. Comparison of Land Use Land Cover Classifiers Using Different Satellite Imagery and Machine Learning Techniques. Remote Sensing, 14(19): 4978. https://doi.org/10.3390/rs14194978.

Chazdon R.L. 2008. Beyond Deforestation: Restoring Forests and Ecosystem Services on Degraded Lands. Science, 320(5882): 1458–1460. https://doi.org/10.1126/science.1155365.

Di Gregorio A. 2005. Land Cover Classification System: Classification Concepts and User Manual. Rome, Food and Agriculture Organization of the United Nations, 208 p.

Di Gregorio A., Jansen L.J.M. 2006. Land Cover Classification System (LCCS): Classification Concepts and User Manual. Rome, FAO, 179 p.

Digra M., Dhir R., Sharma N. 2022. Land Use Land Cover Classification of Remote Sensing Images Based on the Deep Learning Approaches: A Statistical Analysis and Review. Arabian Journal of Geosciences, 15: 1003. https://doi.org/10.1007/s12517-022-10246-8.

Foley J.A., Defries R., Asner G.P., Barford C., Bonan G., Carpenter S.R., Chapin F.S., Coe M.T., Daily G.C., Gibbs H.K., Helkowski J.H., Holloway T., Howard E.A., Kucharik Ch.J., Monfreda Ch., Patz J.A., Prentice I.C., Ramankutty N., Snyder P.K. 2005. Global Consequences of Land Use. Science, 309(5734): 570–574. https://doi.org/10.1126/science.1111772.

Galperin A. 2015. Using of Man-Made Massives in Russian Mining (Engineering: Geological Aspects). Engineering Geology for Society and Territory, 6: 1057–1062. https://doi.org/10.1007/978-3-319-09060-3_192.

Grimm N.B., Faeth S.H., Golubiewski N.E., Redman C.L., Wu J., Bai X., Briggs J.M. 2008. Global Change and the Ecology of Cities. Science, 319(5864): 756–760. https://doi.org/10.1126/science.1150195.

Han H., Li X. 2022. Sustainable Land Use Management in Mining Areas: Challenges and Strategies. Resources Policy, 76: 102616. https://doi.org/10.1016/j.resourpol.2022.102616.

Hu X., Liao W., Wei Y., Wei Z., Huang Sh. 2024. Analysis of Land Use Change and Its Economic and Ecological Value under the Optimal Scenario and Green Development Advancement Policy: A Case Study of Hechi, China. Sustainability, 16(12): 5039. https://doi.org/10.3390/su16125039.

Kong T., Zhang K., Huang L., Di J., Wang Y., Zhang J. 2023. Effects of mixed application of microbial agents on growth and substrate properties of alfalfa in coal gangue matrix with different particle sizes. Journal of China Coal Society, 48(S1): 241–251. https://doi.org/10.13225/j.cnki.jccs.2022.0615 (in Chinese) .

Kou X., Zhao J., Sang W. 2024. Impact of Typical Land Use Expansion Induced by Ecological Restoration and Protection Projects on Landscape Patterns. Land, 13(9): 1513.https://doi.org/10.3390/land13091513.

Lal R. 2004. Soil Carbon Sequestration Impacts on Global Climate Change and Food Security. Science, 304(5677): 1623–1627. https://doi.org/10.1126/science.1097396.

Lambin E.F., Geist H.J. 2008. Land-Use and Land-Cover Change: Local Processes and Global Impacts. Springer Science & Business Media, 222 p.

Lambin E.F., Geist H.J., Lepers E. 2003. Dynamics of Land-Use and Land-Cover Change in Tropical Regions. Annual Review of Environment and Resources, 28(1): 205–241. https://doi.org/10.1146/annurev.energy.28.050302.105459.

Liu H., Wang Q., Liu N., Zhang H., Tan Y., Zhang Z. 2023. The Impact of Land Use/Cover Change on Ecological Environment Quality and Its Spatial Spillover Effect under the Coupling Effect of Urban Expansion and Open-Pit Mining Activities. Sustainability, 15(20): 14900. https://doi.org/10.3390/su152014900.

Liu Y., Li J., Yang Y. 2023. Urbanization and Its Effects on Land Use and Land Cover Change in the Anshan-Benxi Region, China. Journal of Geographical Sciences, 33(2): 245–260. https://doi.org/10.1007/s11442-023-2035-6.

Liu Y., Zhan J., Deng X. 2005. Spatio-Temporal Patterns and Driving Forces of Urban Land Expansion in China During the Economic Reform Era. Ambio: A Journal of the Human Environment, 34(6): 450–455. https://doi.org/10.1579/0044-7447-34.6.450.

Ni J. 2013. Carbon Storage in Chinese Terrestrial Ecosystems: Approaching a More Accurate Estimate. Climatic Change, 119(3): 905–917. https://doi.org/10.1007/s10584-013-0767-7.

Pan Y., Birdsey R.A., Fang J., Houghton R., Kauppi P.E., Kurz W.A., Phillips O.L., Shvidenko A., Lewis S.L., Canadell J.G., Ciais P., Jackson R.B., Pacala S.W., McGuire A.D., Piao S., Rautiainen A., Sitch S., Hayes D. 2011. A Large and Persistent Carbon Sink in the World's Forests. Science, 333(6045): 988–993. https://doi.org/10.1126/science.1201609.

Pang Z., Bu J., Yuan Y., Zheng J., Xue Q., Wang J., Guo H., Zuo H. 2023. The Low-Carbon Production of Iron and Steel Industry Transition Process in China. Steel Research International, 95(3): 2300500. https://doi.org/10.1002/srin.202300500.

Pirnazar M., Haghighi N., Azhand D., Ostad-Ali-Askari K., Eslamian S., Dalezios N.R., Singh V.P. 2021. Land Use Change Detection and Prediction Using Markov-CA and Publishing on the Web with Platform Map Server: Case Study Qom Metropolis, Iran. Journal of Geography and Cartography, 4(1): 7–20. https://doi.org/10.24294/jgc.v4i1.453.

Pontius G.R., Malanson J. 2005. Comparison of the Structure and Accuracy of Two Land Change Models. International Journal of Geographical Information Science, 19(2): 243–265. https://doi.org/10.1080/13658810410001713434.

Post W.M., Kwon K.C. 2000. Soil Carbon Sequestration and Land-Use Change: Processes and Potential. Global Change Biology, 6(3): 317–327. https://doi.org/10.1046/j.1365-2486.2000.00308.x.

Rasskazov I.Y., Arkhipova Y.A., Kryukov V.G., Volkov A.F. 2023. Mining Industry in the Russian Far East: Balancing the Interests of Subsoil Use and the State. Journal of Mining Science, 59(3): 481–489.

Rengma N.S., Yadav M. 2024. Generation and Classification of Patch-Based Land Use and Land Cover Dataset in Diverse Indian Landscapes: A Comparative Study of Machine Learning and Deep Learning Models. Environmental Monitoring and Assessment, 196(6): 568. https://doi.org/10.1007/s10661-024-12719-7.

Seto K.C., Güneralp B., Hutyra L.R. 2012. Global Forecasts of Urban Expansion to 2030 and Direct Impacts on Biodiversity and Carbon Pools. Proceedings of the National Academy of Sciences, 109(40): 16083–16088. https://doi.org/10.1073/pnas.1211658109.

Shelestov A., Lavreniuk M., Kussul N., Novikov A., Skakun S. 2017. Exploring Google Earth Engine Platform for Big Data Processing: Classification of Multi-Temporal Satellite Imagery for Crop Mapping. Frontiers in Earth Science, 5: 1–10. https://doi.org/10.3389/FEART.2017.00017.

Shvidenko A., Nilsson S. 2003. A Synthesis of the Impact of Russian Forests on the Global Carbon Budget for 1961–1998. Tellus B: Chemical and Physical Meteorology, 55(2): 391–415. https://doi.org/10.3402/tellusb.v55i2.16722.

Turner B.L., Lambin E.F., Reenberg A. 2007. The Emergence of Land Change Science for Global Environmental Change and Sustainability. Proceedings of the National Academy of Sciences, 104(52): 20666–20671. https://doi.org/10.1073/pnas.0704119104.

Turner B.L., Skole D., Sanderson S., Fischer G., Fresco L., Leemans R. 1995. Land-Use and Land-Cover Change: Science/Research Plan. IGBP Report, 35: 132.

Verburg P.H., Schot P.P., Dijst M.J., Veldkamp A. 2004. Land Use Change Modelling: Current Practice and Research Priorities. GeoJournal, 61(4): 309–324. https://doi.org/10.1007/s10708-004-4946-y.

Wohlfart C., Mack B., Liu G., Kuenzer C. 2017. Multi-Faceted Land Cover and Land Use Change Analyses in the Yellow River Basin Based on Dense Landsat Time Series: Exemplary Analysis in Mining, Agriculture, Forest, and Urban Areas. Applied Geography, 85: 73–88. https://doi.org/10.1016/j.apgeog.2017.06.004.

Worlanyo A.S., Jiangfeng L. 2021. Evaluating the Environmental and Economic Impact of Mining for Post-Mined Land Restoration and Land-Use: A Review. Journal of Environmental Management, 279: 111623. https://doi.org/10.1016/j.jenvman.2020.111623.

Wu J., Yang J., Ma L., Li Z., Shen X. 2016. A System Analysis of the Development Strategy of Iron Ore in China. Resources Policy, 48: 32–40. https://doi.org/10.1016/j.resourpol.2016.01.010.

Wu Q., Wang L., Wang T., Chen H., Du P. 2024. Global Versus Local? A Study on the Synergistic Relationship of Ecosystem Service Trade-Offs from Multiple Perspectives Based on Ecological Restoration Zoning of National Land Space – A Case Study of Liaoning Province. Applied Sciences, 14(22): 10421. https://doi.org/10.3390/app142210421.

Xu Y., Li J., Zhang C., Raval S., Guo L., Yang F. 2024. Dynamics of Carbon Sequestration in Vegetation Affected by Large-Scale Surface Coal Mining and Subsequent Restoration. Scientific Reports, 14: 13479. https://doi.org/10.1038/s41598-024-64381-1.

Yifter T., Razoumny Yu., Lobanov V. 2022. Deep Transfer Learning of Satellite Imagery for Land Use and Land Cover Classification. Informatics and Automation, 21(5): 963–982. https://doi.org/10.15622/ia.21.5.5.

Zhang X., Liu L., Chen X., Gao Y., Xie S., Mi J. 2021. GLC_FCS30: Global Land Cover Product with Fine Classification System at 30 m Using Time-Series Landsat Imagery. Earth System Science Data, 13(6): 2753–2776. https://doi.org/10.5194/essd-13-2753-2021.

Zhang Z., Bai Z., He Z., Bao N. 2012. Dynamic Changes of Land Use Type and Carbon Sinks Based RS and GIS in Pingshuo Opencast Coal Mine. Transactions of the Chinese Society of Agricultural Engineering (Transactions of the CSAE), 28(3): 230–236. https://doi.org/10.3969/j.issn.1002-6819.2012.03.040.

Zheng L., Li Y., Chen Y., Wang R., Yan S., Xia C., Zhang B., Shao J. 2024. Driving Model of Land Use Change on the Evolution of Carbon Stock: A Case Study of Chongqing, China. Environmental Science and Pollution Research International, 31(3): 4238–4255. https://doi.org/10.1007/s11356-023-31335-5.

Received November 02, 2024;
Revised December 01, 2024;
Accepted December 04, 2024

Поступила в редакцию 02.11.2024;
поступила после рецензирования 01.12.2024;
принята к публикации 04.12.2024

Conflict of interest: no potential conflict of interest related to this article was reported.
Конфликт интересов: о потенциальном конфликте интересов не сообщалось.

INFORMATION ABOUT THE AUTHOR

Lihua Huang, Postgraduate (PhD) student of the Institute of Earth Sciences, Belgorod State National Research University, Belgorod, Russia

ИНФОРМАЦИЯ ОБ АВТОРЕ

Хуан Лихуа, аспирант института наук о Земле, Белгородский государственный национальный исследовательский университет, г. Белгород, Россия